MEASUREMENT AND PREDICTION OF CONTROL VANE FORCE IN THE WAKE OF A SHROUDED PROPELLER SYSTEM

Geon-Hong Kim*, Yeon-Deuk Jeong*, and Seung O Park*
***Department of Aerospace Engineering, KAIST, Republic of Korea**

Keywords: *Shrouded Propeller System, Control Vane, Tail Sitter*

Abstract

For a VTOL UAV such as a tail sitter, providing control forces or moments for attitude control during very low speed ascent, decent or hovering is a critical issue. A plausible solution is to put control vanes in the wake of a propeller. For successful design and operation of these control vanes, control force or moment generated by the control vane should be estimated correctly. In this work, we employ three different numerical methods to estimate the control forces: a potential flow based code, Navier-Stokes solver with momentum source method and moving mesh method. Measurements have also been carried out to get experimental data. It is found that the Navier-Stokes simulation predicts the control force in good agreement with the experimental data while the potential flow method overpredicts the force. Considering the computational time required, however, we find that the momentum source method and the potential based method are more realistic choices than the Navier-Stokes method with moving mesh system.

1 Introduction

Recently UAVs have attracted worldwide attention in both military and civilian purposes. Especially, many VTOL UAVs such as helicopter, multi-rotor, ring-wing and tail sitter type UAVs have been developed for their inherent flexibility in operation since they do not need runway to take-off and land. In this work, we focus on a tail sitter type UAV. In this case, attitude control during a very low speed vertical flight is a serious problem to be resolved. For the tail sitter UAV of the present work, we employ shrouded propeller system as a pusher type thruster. In this case, an efficient way to provide attitude control force and/or moments at very low flight speed is required to utilize propeller wake stream.

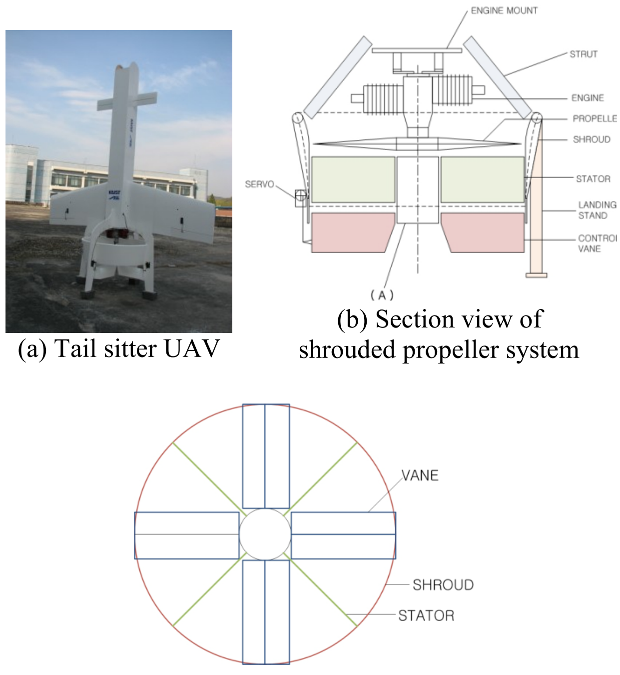

(a) Tail sitter UAV

(b) Section view of shrouded propeller system

(c) Top-down

Fig 1. Tail sitter type UAV designed at KAIST and shrouded propeller system used in the tail sitter

The shrouded propeller system(SPS) of the present work is shown in figure 1. The system consists of shrouded propeller, stators and four control vanes. The control vanes are installed near the exit of the shroud and generate control forces owing to wake stream. To predict control forces accurately, the performance of the shrouded propeller induced flow should be simulated correctly.

A shrouded propeller in comparison with an unshrouded one is well known since the pioneering work of Ref. 1. However, studies on aerodynamics of the control vanes placed as shown in figure 1 are rather rare as can be found in Ref. 2.

In this paper, we perform numerical simulation of the shrouded propeller system including the stator and the control vane in three different ways; potential flow based method, momentum source method, and moving mesh method. And the results are compared to the experimental results.

2 Numerical Simulations

2.1 Geometric Configuration

We first present a brief summary of geometric configuration of the shrouded propeller system(figure 1(b)) consisting of a propeller, shroud, stators and control vanes. The cross section of the shroud is of airfoil shape. The inner diameter of the shroud is 0.668m. Four stators are placed crosswise right behind the propeller to offset torque caused by rotating propeller and engine. Each stator is a rectangular wing whose cross section is the CH10 airfoil and the chord length and the span are 77mm and 278mm, respectively.

Four control vane units are installed next to the stators, each unit being at 45 degrees to a stator plane as sketched in figure 1(c). One control vane unit is made of triplanes of three identical wing segments and cross section of this wing segment is of NACA 63(1)-012 airfoil. The gap between adjacent wing segments is 60mm. The chord length and the span are 100mm and 278mm, respectively. The reason for making each control vane unit be composed of triplanes is simply to provide sufficient control force under given geometric constraint.

For the present tail-sitter UAV, we just employ a commercially available 2-blade wood propeller whose diameter is 26 inches and pitch is 8 inches. The details of the geometric data from the supplier were not available. As we need the geometric data for numerical simulation of aerodynamics, we performed a 3D scan of the propeller to get the geometric data. Figure 2 illustrates this process. From the geometry of propeller, we find the chord and blade angle distributions of the propeller as shown in figure 3.

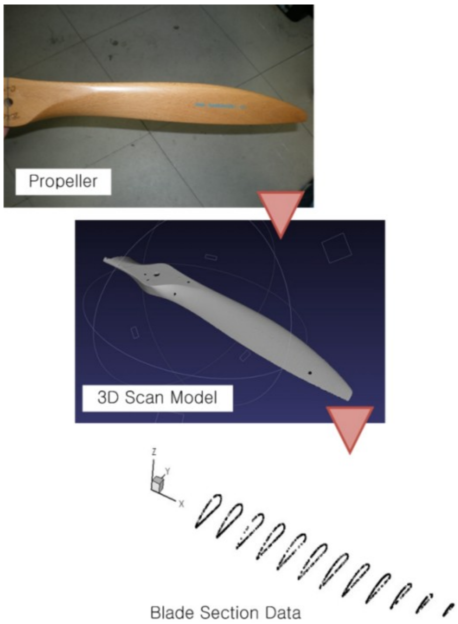

Fig 2. Procedure to obtain blade geometry data

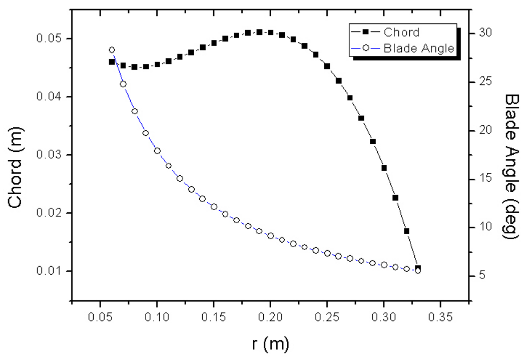

Fig 3. Chord and blade angle distribution of propeller

2.2 Potential Flow Based Method

As commented briefly already, we adopted three different methods for numerical simulation. One of them is a potential flow based method, which we describe in this section. We employed the DFDC(Ducted Fan Design Code)[4] to simulate the shrouded propeller and AVL[5] to estimate control forces generated by control vanes which are placed near the exit of shroud. The two codes are open source codes released by Mark Drela and his group.

In DFDC, a shroud(or duct) is represented by axisymmetric panels and the rotor blades are represented by lifting lines. The induced velocities associated with blade-row loading are represented by vortex sheets shed into the flow field. Blade elements models are used for blade row sections using two-dimensional lift, moment and profile drag characteristics to account for loading and viscous losses[6]. Figure 4(a) illustrates the computation model of the shrouded propeller used in the present work. AVL is a code for the aerodynamic and flight dynamic analysis of rigid body by using vortex lattice method for the lifting surface. Figure 4(b) shows the computational model of stators and control vanes for the AVL program used in the present work. We employed these two codes in a rather privative and very loosely coupled manner as stated below.

1) Using DFDC, we obtain the velocity distributions behind the propeller as if there were no stator and control vanes in the downstream region.

2) By using velocity distributions of step 1 as inlet free stream flow conditions, we use AVL to estimate control forces due to control vane units.

Since the inlet free stream flow from step (1) is not uniform, we simply take the freestream velocity components at a spanwise station corresponding to each control point to formulate the zero normal velocity condition.

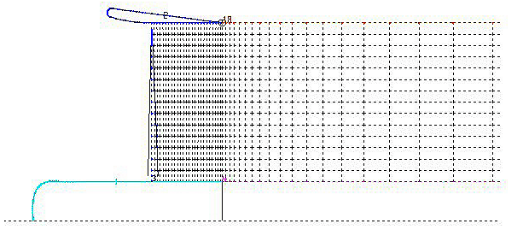

(a) Shrouded propeller model for DFDC

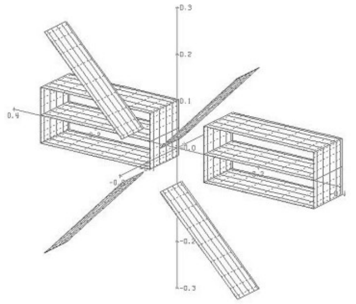

(b) Analysis model of stators and control vanes for AVL(two control vane units omitted for simplicity)

Fig 4. Aerodynamic analysis model of a shrouded propeller and a control vane

2.3 Navier-Stokes Solver

For a more accurate computation of control forces, we employ a full Navier-Stokes solver. We used the FLUENT as the Navier-Stokes solver. We take two different ways to simulate the aerodynamics of the propeller. One is the momentum source method in which the propeller is replaced by the momentum source generator in the computation domain. The other is a moving mesh method where the flow around the propeller is directly computed with a mesh system rotating with the propeller embedded in a full stationary computational domain.

2.3.1 Momentum Source Method

In the momentum source method, the propeller was modeled as a disk providing momentum to the flow passing through the disk. The additional momentum is added to the momentum equations in x, y, and z directions as a source term. In FLUENT, such a source term can be added via UDF(user defined function) which is written in C/C++ language[7].

Momentum source term at a radial station can be estimated by dividing the force at the station by volume of a ring whose radius *r* is the distance from center of disk to the station as follows.

$$\vec{f}_i = \frac{\vec{F}_{bem}}{2\pi rtdr} \quad (1)$$

where $\vec{F}_{bem}$ is a vector of aerodynamic forces calculated using BEM(Blade Element Method) at a given radial station and t is the thickness of the propeller disk.

BEM, as is well known, is a method for analysis of rotor by breaking a blade down into many two-dimensional parts(blade elements).

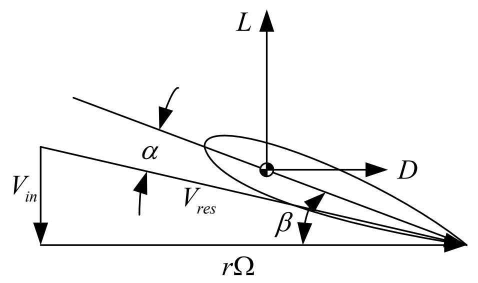

Fig 5. Lift and drag generated by a propeller section

Figure 5 demonstrates lift and drag generated by a blade element at hovering flight condition.

As we are interested in control forces generated by control vanes at very low vertical speed flight, the hovering condition is reasonable for the present simulation. As can be seen from figure 5, estimation of the induced velocity V_{in} and C_l and C_d of the airfoil section is essential to calculate L and D. The induced velocity V_{in} , for a given radial location(see Eq.(2)) evolves from the Navier-Stokes simulation as the iteration progresses. We take the average of vertical component velocities of all the grid points at a given radius at the disk plane to get V_{in}.

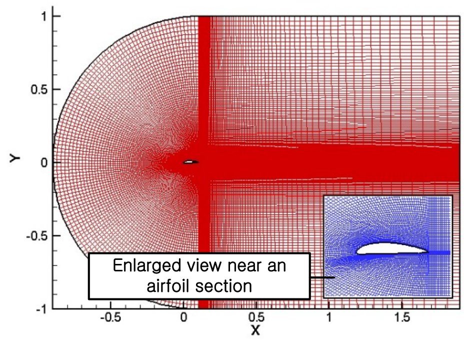

Fig 6. Grid for aerodynamic analysis of propeller section at radial station of 220mm from center

C_l and C_d of each 2D blade element of the propeller are computed by solving the 2-D Navier-Stokes prior to the present momentum

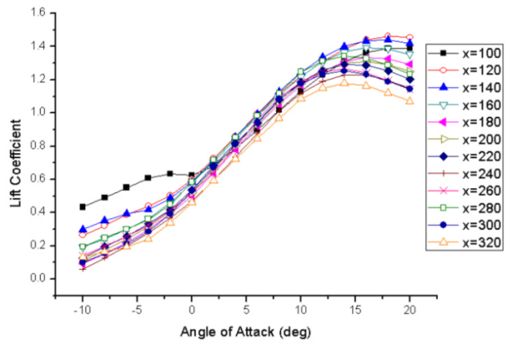

(a) Lift coefficients

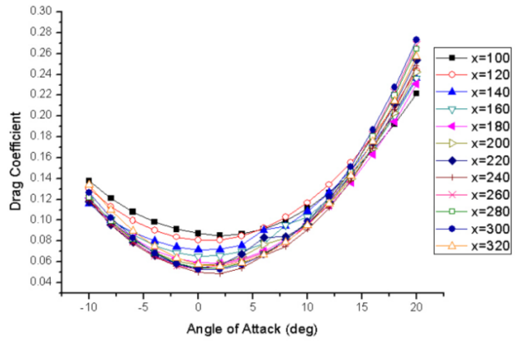

(b) Drag coefficients

Fig 7. Lift and drag coefficients of propeller sections.

source method calculation. The collection of C_l and C_d obtained from the look-up table. The 2D Navier-Stokes computation was done again by using the FLUENT with the SST k-omega turbulence model. Figure 6 illustrates the computational grid for 2D calculation.

Computations were carried out at 12 sections between 100mm and 320mm from the center of propeller along the radial direction with increments of 20mm. Reynolds numbers were set to be the local Re number based on chord length at each section when the propeller rotates at 4000rpm. The lift and drag coefficients with respect to angle of attack are shown in figure 7.

Figure 8(a) shows the computational domain and boundary conditions for the momentum source method. Structured grid system was used for the disk plate only and the other domains were constructed by using tetrahedral meshes. The grid around the shrouded propeller system is shown in figure 8(b). Figure 8(c) and (d) show the grid of propeller disk and near stators and a control vane, respectively. The computation domain consisted of about 2 million meshes and SA model was used as the turbulence model.

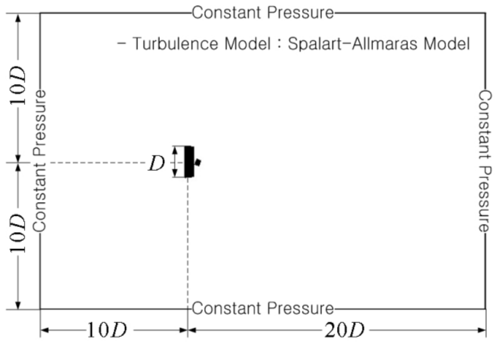

(a) Computational domain and boundary conditions

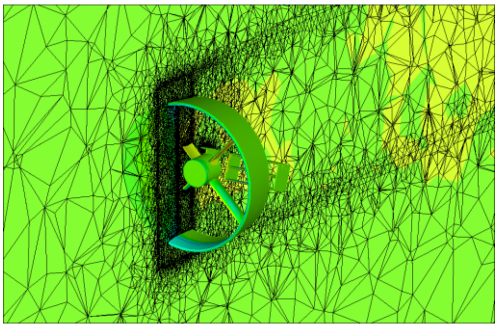

(b) Grid near shrouded propeller system

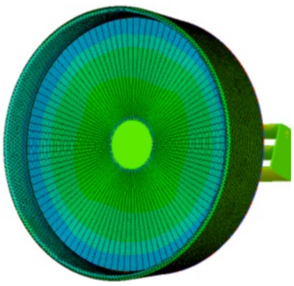

(c) Grid of the propeller disk

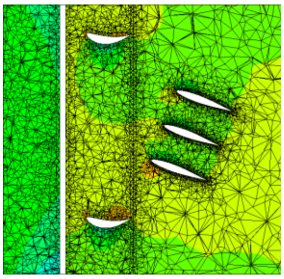

(d) Grid near stators and control vanes

Fig 8. Computational domain and grid arrangement near the shrouded propeller system.

2.3.2 Moving Mesh Method

In the moving mesh method, we employ two different computational domains: rotating domain where the propeller geometry is contained and stationary domain enclosing the rotating domain and the other solid body components such as the shroud, the stators, and the control vanes. Figure 9(a) shows the grid system near the SPS. For the simulation, unsteady computation was done with the time step size corresponding to the time required for the propeller to rotate 1 degree.

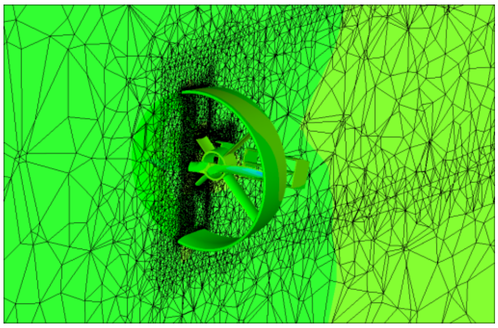

(a) Grid around SPS

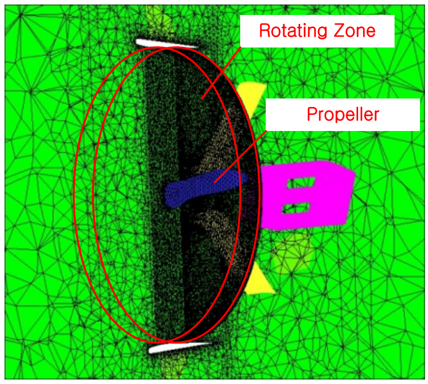

(b) Grid near propeller for moving mesh. Shroud is omitted in this figure to clarify the rotating zone.

Fig 9. Grid arrangement near SPS for moving mesh method.

3 Experiment

The control forces due to control vanes were measured by a measurement system as shown in figure 10.

The SPS was hung like a pendulum as shown in figure 10(c). The model and the supporting frame were connected by ball joint in order to make the SPS swing freely. When control forces were exerted on control vanes then the model was tilted and balanced with an angle of θ. To estimate the forces generated by control vanes, we used the following simple relation.

$$F_v = \frac{L}{L + L_v} \times W \sin\theta \qquad (2)$$

where F_v is the control force that we want to measure. W represents the weight of the SPS

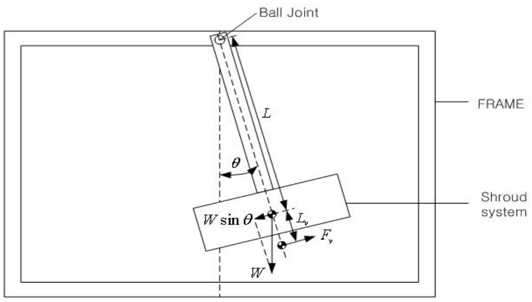

(a) Schematic representation of experimental setup

(b) Measurement system (c) Experiment model

Fig 10. Set up for experiment on SPS to measure control forces.

which is a known value and L_v is the distance from the center of mass of the SPS to the aerodynamic center of control vanes. L is the distance from the center of rotation to the center of mass of the SPS which can be estimated simply by[9],

$$L = \left(\frac{\tau^2}{2\pi}\right) g \tag{3}$$

where τ is the period of the simple pendulum motion of the system, which is measured easily

The angle θ was measured using the slope sensor TILT SA1[10].

The calibration for the slope sensor is given in figure 11.

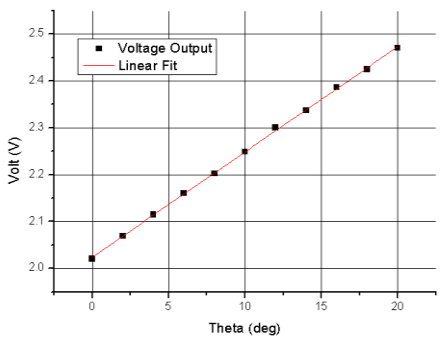

Fig 11. Result of sensor calibration

4 Results and Discussion

Computations and measurements of control forces were done at various control vane deflection angles and rotating speed of the propeller. The deflection angles were varied from 0 deg to 20 deg which is the operation limit angle of the control vane. The rotation speed of propeller were varied from 2500 rpm to 4000 rpm with increment of 500 rpm.

The forces, predicted and measured, were non-dimensionalized by the following equation.

$$C_{F_v} = \frac{F_v}{\frac{1}{2}\rho (nD)^2 S_{vane}} \tag{4}$$

where n is the rotating speed of propeller in rps, D is the inner diameter of the shroud, and S_{vane} is area of the control vanes. The results are shown in figure 12.

As can be seen from the figure, the predictions from the three different methods are in good agreement with the experimental data. We comment here that the predictions at different rpms collapsed into one curve as presented in the figure, while the experimental data scattered widely. We see a general tendency that the potential flow based prediction overpredicts the force compared to the Navier-Stokes predictions. It took only a few seconds of CPU time for the potential flow based method. When FLUENT with momentum source method was used, the computation of a case took about 6 CPU-hour with AMD Phenom 9950 processors which clock at 2.61GHz. In the

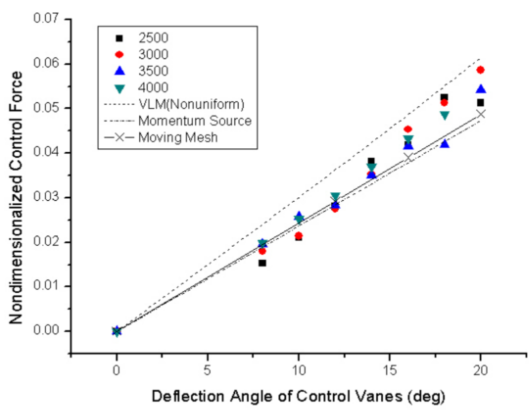

Fig 12. Control force variation with respect to deflection angles.

case of moving mesh method, computations over 20 revolutions of propeller were required to get converged solution. Parallel FLUENT computing was done using a cluster server who has 16 nodes of Intel Xeon X5550 CPU clocked at 2.66GHz and it took about 5 days to obtain control forces per one case. The results of the moving mesh method are only slightly higher than those of the momentum source method with no significant differences between the results of two methods. We thus find that the momentum source method and the potential flow based method are good chices for the prediction at a design stage.

5 Concluding Remarks

To predict control forces generated by control vanes, we adopted three different methods to analyze the aerodynamics of control vanes numerically: potential flow based method, momentum source method, and moving mesh method. Experiments were also carried out to validate the numerical methods.

Based on the comparison of the results and computational time required, we find that the potential flow based method and the momentum source method are practical choices of simulation at a design stage.

6 Acknowledgement

The authors gratefully acknowledge the support from UTRC(Unmanned Technology Research Center) at KAIST(Korea Advanced Institute of Science and Technology) originally funded by DAPA, ADD.

References

[1] Platt R.J., "Static Tests of a Shrouded and an Unshrouded Propeller," NACA RM No.L7H25, 1948

[2] Guerrero I, Londengerg K, Gelhausen P, and Myklebust A, "A Powered Lift Aerodynamic Analysis for the Design of Ducted Fan UAVs," 2nd AIAA Unmanned Unlimited Systems, Technologies , and Operations – Aerospac, 15-18 September 2003, San Diego, California

[3] Menter F.R., "Two-Equation Eddy-Viscosity Turbulence Models for Engineering Applications," AIAA Journal, Vol.32, No.8,pp.1598-1605, 1994

[4] DFDC, http://web.mit.edu/drela/Public/web/dfdc/

[5] AVL, http://web.mit.edu/drela/Public/web/avl/

[6] Drela M., "Axisymmetric Analysis and Design of Ducted Rotors," Theory document of DFDC

[7] Fluent Inc., *FLUENT 6.3 UDF Manual*, 2006

[8] Gu H. and Kinnas S.A., "Modeling of Contra-Rotating and Ducted Propellers via Coupling of a Vortex-Lattice with a Finite Volume Method," Propellers/Shafting 2003 Symposium, Sep 17-18, 2003

[9] Beer F.P. et al., Vector Mechanics for Engineers, Dynamics, 7th Edition, McGraw Hill, 2005

[10] DAS Technology, http://www.das-co.com

Contact Author Email Address

Geon-Hong Kim : kgb3233@kaist.ac.kr
Yeon-Deuk Jeong : ydjeong@fdcl.kaist.ac.kr
Seung O Park : sopark@kaist.edu

Copyright Statement